International Journal of Emerging Engineering Research and Technology
Volume 8, Issue 6, 2020, PP 32-43
ISSN 2349-4395 (Print) & ISSN 2349-4409 (Online)

Transition of Flow past a Square Rod through Passive Control Method at Low Reynolds Number

Raheela Manzoor[1*], Aneela Anwar[1], Shams-ul-Islam[2] and Khurshid Jamil[1]

[1]*Mathematics Department, SBK Women's University Quetta, Pakistan*
[2]*Mathematics Department, COMSATS University of Information Technology, Islamabad, Pakistan*

***Corresponding Author:** Raheela Manzoor, Mathematics Department, SBK Women's University Quetta, Pakistan*

ABSTRACT

Numerical simulations are performed in order to investigate the variation of flow behavior and force coefficients of the flow past a square rod with two detached control rods. A two-dimensional numerical code is developed using the lattice Boltzmann method (LBM). Firstly, the effect of grid independence computation is studied for the flow past a single square rod to check the adequacy and grid points. After that, the simulations are further performed to investigate the effect of lower Reynolds number (Re) at different gap spacing (g). The gap spacing is chosen in the range g = 1-4 and Re is selected within the range Re = 1-75. Three different flow modes, i) Steady flow, ii) Shear layer reattachment and iii) Unsteady flow modes are found in this study with successive increment in Re at fixed value of gap spacing. The steady flow behavior is observed at g = 1, 3 for Re = 1-70, at g = 2 for Re = 1-75 and g = 4 for Re = 1-60, Shearlayer reattachment flow mode is occurred at g = 3 for Re = 75. While, unsteadiness in flow is observed only at g = 1 for Re = 75 and g = 4 for Re = 70 and 75. In physical parameters, Cdmean, Cdrms, Clrms and St values are calculated and compared with single rod data. The maximum value of Cdmean is 5.5909, where existing flow mode is steady. The minimum value of Cdmean is 0.5293. The root mean square values of drag and lift are containing smallest values than single rod data. The maximum value of Strouhal number is obtained at g = 1 for Re = 75 which is 0.1049.

Keywords: *Strouhal number, Vortex shedding, Cdmean, Reynolds number, Gap spacing.*

INTRODUCTION

Flow behavior around a bluff body, when it flows over it got the attention of several researchers due to its practical engineering applications related to blunt objects upon which anyone may see propagation of fluid over these objects like road, water and air transport, automobiles, air-cool machines, etc. Most of the research work based on bluff bodies is related to study of flow induced vibrations, their resulting effects on the structures, dependence of wake modes and aerodynamic force characteristics on different parameters like Reynolds number (Re = $U_\infty d/\nu$) and gap spacing (g = s/d, where s is the distance and d is size of rod) between the structures, as well as size and shape of structures.

Various applications of bluff bodies can be found in cooling towers, cable suspension bridges, high rise buildings, heat exchangers etc. Many experimental and numerical studies are performed for the analysis of wake structure using different techniques. The main adopted techniques are passive control and active control methods. In active control method (ACM) the forces are controlled by supplying energy externally, while in passive control method (PCM) the forces are controlled by surface roughness and by changing the size and shape of rod named as control plate or control plate. Passive control method as compared to active control method is cheaper and easily applicable. Mansingh and Oosthuizen, (1990) experimentally studied the control plate effect placed downstream of a rectangular rod for different plate lengths over a range of Reynolds numbers from 350 to 1150. They found that the Strouhal number decreases in presence of downstream control plate. An experiment is conducted through Sakamoto *et al*., (1997) for reduction of fluid forces. They examined different stream wise arrangement of main circular rod and control rod and obtained the maximum reduction at Re = 6.5×10^4 in Cdrms and Clrms, when control rod is placed at a distance 0.06d - 0.14d and 0.14d - 0.16d at an angle of 60^o and 120^o, respectively. The amplitude of transverse force was investigated by Dalton *et al*., (2001) using computational

method and fluid propagation is studied at three different Reynolds = 100, 1000 & 3000. Small control plate showed the effect at main object by considering the appropriate gap between main rod and control rod. The lift force is seemed to be reduced at large amount also drag force reduced with excellent percentage. Numerical computations are done through Mittal, (2003) to better understand the effect of slip control plate in the wake region of circular rod for Re = 100. It is found that the shortest length of control plate is required to suppress vortex shedding is two times the diameter of rod, and needs to be placed in basic unperturbed part of wake region. The upstream edge of plate is located very close to the wake region where vertical velocity component changes its direction. So as compare to the downstream edge, the upstream edge has much more significant effect on the unsteadiness of the flow. Flow over circular rod in presence of dual control plates is numerically investigated by Hwang and Yang, (2007) in order to reduce the drag force on rod. Splitters plates are placed in center line horizontally in 2-D channel. G_1 and G_2 are the gap spacings between circular rod and dual control rods. It is observed that upstream control plate reduces the stagnation pressure, while downstream plate increases the base pressure by suppressing vortex shedding. This combination causes the remarkable drag reduction on circular rod. The reduction of vortex shedding is experimentally investigated for fluid flow around square object for the limitation of Re up to two digits by Shao and Wai, (2008). The observations were occurred in the form of non-satisfied results, after that they improved their arrangement and used small control circular or square rods or small narrow strip within, $1.12x10^4 < Re < 1.02x10^5$. Their experimental results showed that complete vortex shedding depends upon bluffness of the body that is square rod. Ali *et al*., (2010) numerically simulated the generation of aeolian at low Reynolds number and low Mach number for flow past a single square rod(SSC) attached with thin control plate. The length of plate is selected from L = 0.5d to 6d and three different flow modes are identified for finding levels of aeolian tone. A numerical study is carried out at Re =150 with and without control plates by Ali *et al*., (2011) to study the flow structure. The length of control plate is varied form 0.5d to 6d. It was found that length of plate produced the strong vibrations towards exit side of the channel and the suitable length of plate is found from L = 0.5d to 4d.Perumal *et al*., (2012) performed numerical simulations by employing Lattice Boltzmann Method (LBM). The observations are gained in terms of distinct stoppage ratios. At high stoppage, flow periodicity is occurred at Reynolds number greater than or equals to 10. The authors observed that faster periodic manner is experienced by elongated the width of L_d of channel and by setting the object close to the inlet of the channel. Wu *et al*., (2012) studied the vortex induced vibration suppression of a deep water riser by multiple control rods through an experiment. They considered four identical small circular cylinders attached with the main circular cylinder at Re = 2400 - 7600. An effective impact of upstream control plate in presence of rectangular rod was numerically studied by Malekzadeh and Sohankar, (2012) at different widths of control plate for various values of Reynolds number. Hence 86% of reduction is observed in fluid vibrational forces at Re = 160 for g = 3. Golani and Dhiman, (2014) performed numerical computations to simulate flow around a circular rod by using FVM at the range of Reynolds number from 50 to 180 and discussed Cdmean and Strouhal values. It was concluded that Cdmean decreases by increasing Reynolds number. Besides this, Cdrms and Clrms coefficients and St has been observed being increased with further increment in Reynolds number. Liu *et al*., (2014) conducted numerical study under the influence of g, d, Re and θ regarding to check to the control of vortex vibrations when the fluid propagates over round object that is attached with small circular rod. Authors found four flow behaviors and become able to study fluid forces reduction and observed that drag and lift are increased at $\theta = 0^o$. When the angle of attack is increased the frequency magnitude if Cdmean decreased. The presence of one control rod at upstream, downstream and at both upstream and downstream adjustments of control plates is numerically examined by Vamsee *et al*., (2014) for low Reynolds numbers of an incompressible flow equations and MAC principles. It is observed that control rod placed at upstream position has an excellent contribution in order to decrease the vibrational forces and has small impact for controlling vortex shedding. The percentage reduction for Cdmean in fluid vibrations using dual configuration is observed by Barman and Bhattacharyya, (2015)to study the existence of control plate that attached to a SSC by the implementation of control volume method over an oriented settlement of grids. It is examined that as the rod length is taken smaller that is 1.5 times less than the length of the object and reduction take place in drag force, the

upstream rod has minor impact on amplitude of Clrms. A numerical investigation is done for the drag and lift reduction for flow past a square rod in presence of different thorn lengths at different angles by Dey and Das, (2015) for Reynolds number, Re = 100-180. The authors found that the reduction of drag and lift coefficient are directly proportional to thorn length and thorn inclination angle. They observed 16% and 22% drag reduction for Re = 100 and 180, respectively.

Two dimensional numerical simulations are studied to observe the flow behavior on a single square rodby Nidhul *et al*., (2015)with and without corner cutting edges with the consideration of FVM at Re = 150. It is found that the Shearlayer for SC with-out corner modification is delayed. They found maximum reduction of vortex induced vibration responses. Islam *et al*., (2017) placed three control cylinders in upstream location and three at downstream location of a square cylinder and studied the effect of Reynolds number and gap sapcings. They found weak vortex shedding, steady and strongly induced vortex shedding flow patterns. For Reynolds number Re = 160 a numerical study is conducted by Shams *et al*., (2017) in 2-D to reduce the strong vibrating forces when fluid past over square rod in the attachment of upstream, downstream and dual control plates. Lengths of plates are varied as $1 \leq L \leq 4$ and gap spacings are taken as $0 \leq g \leq 7$. It is found that maximum percentage reduction is occurred for dual control plates.

From all above mentioned literature, it is cleared that much attention is paid to study the flow behavior and to control fluid forces through passive control method by using single or multiple control rods at large range of Reynolds number. Very less work is done by using range of Re > 100. In present study we focused on low range of Reynolds numberi.e Re = 1-75 to study the flow structure mechanism at different values of gap spacing in presence of detached dual control rods using single relaxation time lattice Boltzmann method (LBM).

The outline of paper is arranged as follows. Section 2 concerns with statement of problem and boundary conditions, Numerical method is described in Section 3. Section 4 is devoted for grid independence study and computational domain. The analysis of Reynolds number at different gap spacings on the aerodynamic forces are presented in Section 5 and finally, in Section 6, conclusions are drawn.

Statement of Problem and Boundary Conditions

The proposed problem used to investigate and anaylize the computational complexities using the lattice Boltzmann method for two-dimensional (2-D) laminar flow past a square rod which is symmetrically placed with respect to channel centerline in a channel detached with control rods, as shown in Fig. 1. The size of the main rod is d and control rod is d1 in a channel of length L and height H. Lu is the upstream location of the computational domain and Ld is the distance behind the main rod. At entrance, the parabolic velocity profile ($\boldsymbol{u} = 1.5\boldsymbol{U}_\infty (1-y/H^2, \boldsymbol{v} = 0$) is adopted (Guo *et al*., 2008). At the outlet boundary, the convective boundary condition ($\partial_t \boldsymbol{u} + \boldsymbol{u}_\infty \partial_x \boldsymbol{u} = 0$) is applied in terms of distribution functions (Breuer*et al*., 2000). At solid surfaces, including the surface of control rods, main square rod and walls of channel, the bounce back rule is used, that is referred as no slip boundary condition (Guo *et al*., 2008).The momentum exchange method is used to calculate the forces on the rod (Yu *et al*., 2003).

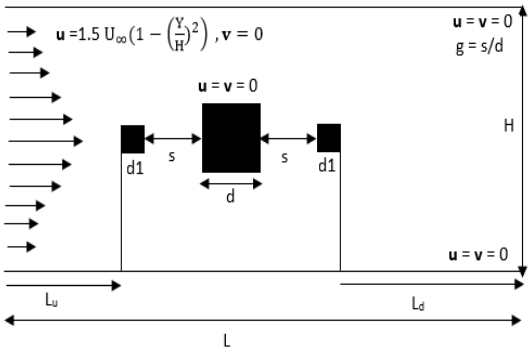

Fig1. *Schematic diagram for flow over a square rod detached with upstream-downstream control rods.*

Lattice Boltzmann Method

We have used lattice Boltzmann method (LBM) for the numerical simulations performed for the present study. LBM has several advantages over the traditional computational methods like finite difference method, finite element method and finite volume method. The parallelization of computer code is easy for LBM due to the local nature of its collision and streaming steps (Wolf-Gladrow, 2005). LBM is explicit in nature and second order accurate both in space and time (Wolf-Gladrow, 2005; Mohamad, 2011) and also the pressure term is calculated using the equation of state (Mohamad, 2011).The discretized lattice Boltzmann equation is

$$f_i(\mathbf{x} + \mathbf{e_i}, t + 1) = f_i(\mathbf{x}, t) - \frac{1}{\tau}\left[f_i(\mathbf{x}, t) - f_i^{eq}(\mathbf{x}, t)\right] \quad (1)$$

Where $f_i(\mathbf{x}, t)$and $f_i^{eq}(\mathbf{x}, t)$ are distribution and equilibrium distribution functions and τ is the single-relaxation time parameter. The equilibrium distribution function is defined as:

$$f_i^{eq}(\mathbf{x}, t) = w_i\rho\left[1 + \frac{3(\mathbf{e_i}.\mathbf{u})}{c_2} + \frac{4.5(\mathbf{e_i}.\mathbf{u})2}{c4} - \frac{1.5\mathbf{u}2}{c_2}\right] \quad (2)$$

The weighting coefficients (w_i) for the nine-velocity of two-dimensional model are

$$w_0 = 4/9, \quad (3a)$$

$$w_1 = w_2 = w_3 = w_4 = 1/9, \quad (3b)$$

$$w_5 = w_6 = w_7 = w_8 = 1/9, \quad (3c)$$

The macroscopic density ρ and momentum ρ**v** in a cell are calculated as:

$$\rho = \sum_{i=0}^{8} f_i, \rho\mathbf{v} = \sum_{i=1}^{8} f_i\mathbf{e}_i \quad (4)$$

The kinematics viscosity is defined as:

$$\nu = 1/3(\tau - 0.5) \quad (5)$$

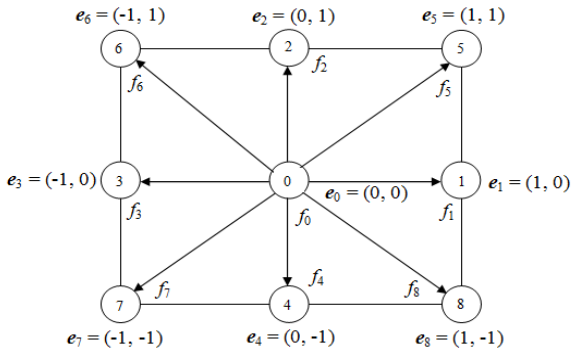

Fig2. *D2Q9 particles direction*

COMPUTATIONAL DOMAIN AND GRID INDEPENDENCE STUDY

A suitable segment of computational domain has great importance in order to study flow around any bluff body. Therefore, it is essential to choose appropriate length of upstream distance Lu, downstream distance Ld and height H of computational field. So, to study the effect of computational domain, we have chosen three different values of Lu, Ld and H for g = 1 and Re = 75 and the computed values of Cdmean, Clrms and St shown in Table 1. The obtained results in terms of Cdmean, Clrms and St are approximately. First attempt is carried out for distinct Lu = 7d – 9d by fixing Ldand H that is Ld =33d, H = 9d. The physical parameters Cdmean and Clrms showed higher values at Lu= 8d, while St has small value as compared to other coefficients.

Next Ld and H are varied from 33d- 35d and 9d-11d respectively. It is noticed that if we consider, Lu = 8d; Ld = 35d; H = 11d, it take much computational time because of more grid points as compared to other cases. Because, all the force coefficients Cdmean, Clrms and St have maximum values as compare to the other cases Table1. It is observed that when lengths are taken as Lu = 8d, Ld = 33d and H = 11d Cdmean, Clrms and St showed some good sensation regarding to their values. No matter we consider any one case from all mentioned cases except Lu = 8d; Ld = 35d; H =11d. Therefore, we simulate present problem by taking Lu = 8d; Ld = 33d; H=11d.

Table1. *Domain independence study at g = 1 and Re = 75*

Cases	Cdmean	Clrms	St
Lu = 7d; Ld = 33d; H = 11d	0.5656	0.0440	0.1621
Lu = 8d; Ld = 33d; H = 11d	0.5908	0.0471	0.1591
Lu = 9d; Ld = 33d; H = 11d	0.5684	0.0452	0.1561
Lu = 8d; Ld = 31d; H = 11d	0.5707	0.0455	0.1591
Lu = 8d; Ld = 35d; H = 11d	0.5706	0.0455	0.1592
Lu = 8d; Ld = 33d; H = 9d	0.5482	0.0435	0.1591
Lu = 8d; Ld = 33d; H = 13d	0.5908	0.0471	0.1621

The main aim of computational fluid dynamics (CFD) is to replace the continuous problem domain with a discrete domain by using grid independence phenomenon. The whole comp-utational investigations are depending on the size of the main object that is placed in the channel. In this phenomenon the surface of the object is partitioned into various cells that contain different numbers of grid point. In this regard, we have taken three cases for different grid points (10d, 20d and 24d) comprises of (Xmax, Ymax) = (421, 111), (841, 221) and (1018, 265).

We have calculated the values of force statistics Cdmean, Cdrms, Clrms and St at these selected grid points shown in Table 2. All values of force statistics have higher magnitudes at d = 10 and having minimum magnitudes at d = 20. We will not select d = 10, for present simulation. At d = 30, the grid points along x and y-axis are increased as compared to d = 20 and also at d = 30 grid points, computationally the investi-gations are costly because it require much time to complete simulation. It is noticed that at d = 20 the accurate values of force coefficients are

occurred see Table 2. So we have selected d = 20 grid points as the size of rod for this present problem. Guo *et al*., (2008) also selected (20d) grid points for his simulation.

RESULTS AND DISCUSSIONS

Two dimensional numerical study is conducted for flow past over a square rod in presence of two detached control rods at fixed value of gap spacing by varying the Reynolds number in order to investigate the study and unsteady behavior of flow. The results are obtained in terms of vorticity contour visualization, drag and lift coefficients and force statistics.

Table2. *Grid independence study for flow past over a square rod*

Cases	Cdmean	Cdrms	Clrms	St
d = 10	1.5621	0.0291	0.3518	0.3097
d = 20	1.5172	0.0246	0.3052	0.1914
d = 24	1.5328	0.0408	0.3092	0.2209

Analysis of Flow Modes

During the investigations the different flow behaviors such as steady, Shearlayer reattachment and unsteady flow modes are observed by fixing g and by varying Reynolds number. The brief look of existence of these respective flow modes are presented in Table 3.

Table3. *Existing flow modes at fixed value of g at different Re*

Flow Mode	(g, Re)
Steady flow mode	g = 1, Re = 1, 5, 10, 15, 20, 30, 40, 50, 55, 60, 70 g = 2, Re = 1, 5, 10, 15, 20, 30, 40, 50, 55, 60, 70, 75 g = 3, Re = 1, 5, 10, 15, 20, 30, 40, 50, 55, 60, 70 g = 4, Re = 1, 5, 10, 15, 20, 30, 40, 50, 55, 60
Shearlayer reattachment flow mode	g = 3, Re = 75
Unsteady flow mode	g = 1, Re = 75, g = 4, Re = 70, 75

Steady Flow Mode

The flow is seemed to be steady when gap spacing is fixed at g = 1-4 and Reynolds number is varied at from Re = 1, 5, 10, 15, 20, 30, 40, 50, 55, 60, 70, respectively. Fig. 3(a-d) is showing the vorticity behavior of steady flow at g = 1. The flow made a single whole loop on all the three objects, which showed that only one object is placed in computational channel clear from Fig. 3(a). When Re is taken within the range Re = 5- 70 the flow is propagated towards downstream side of the domain with lengthened wake region (see Fig. 3(b-d). That is the wake region is seemed to be larger and larger with increasing Reynolds number.

Vorticity contour analysis of steady flow for g = 2 at Re = 1-70 is shown in Fig. 3(e-f). As gap is fixed at g = 2, the fluid is flowing in little bit different style as compared to g = 1at Re = 1. The flow attached directly to main rod after passing over the upstream control rod, main rod and then downstream control rod. The wake region is not appeared at Re = 1 (seeFig. 3(e)). When Reynolds number is varied from Re = 5 - 75 the steady flow is observed with larger wake region shown in Fig. 3(f).

Vorticity contour analysis for g = 3 and 4at Re = 1-70 is shown in Fig. 3(g-j). It is observed that at g = 3 and Re = 1 and g = 4 at Re = 1and 5, the flow made separate loops on every object placed in 2-D channel clear from Fig. 3(g, h), which predict, that there is no effect of both up and down stream control rods on the main rod and there is no need to place the control rod. As Re increased from Re > 1, fluid is flown towards main and downstream control rod. Therefore, when Re = 5- 70 flow is seemed to be reattached directly to the main rod and then to the downstream control rod with lengthened wake region shown in Fig.3(i-j). No disturbance is observed at the exit side of the channel.

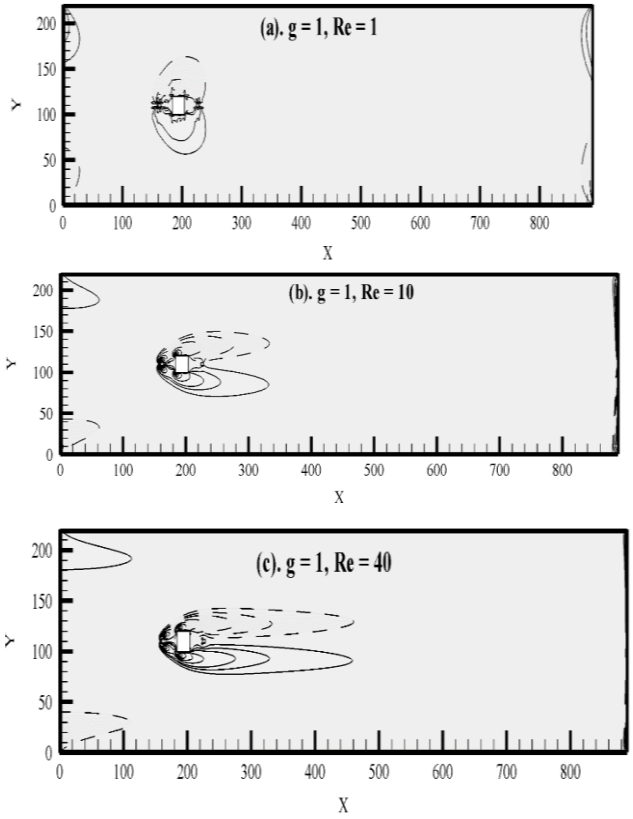

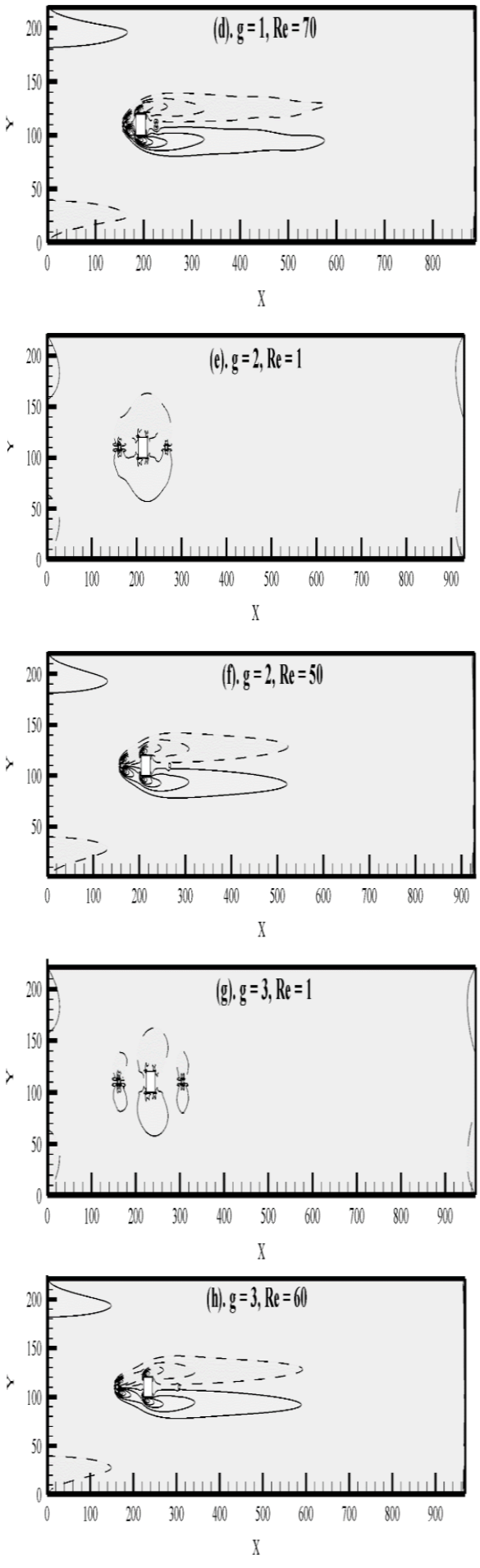

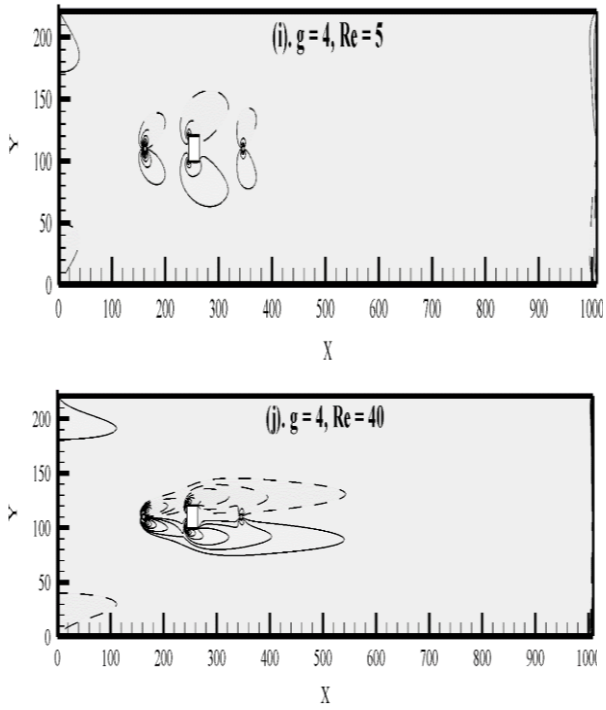

Fig3(a-j). *Vorticity contours visualization for steady flow mode g = 1-4 for Re = 1-75.*

Shearlayer Reattachment Flow Mode

Next flow mode is Shearlayer reattachment that is observed at g = 3 for Re = 75. In present study g = 3 is supposed to be moderated gap spacing, that slightly disturbed the steady flow with larger wake region and vortices are generated with weaken strength , which is cleared from Fig. 4(a)and are not energetic so the flow is named as Shearlayer reattachment flow mode. Time-history of Shearlayer reattachment flow mode is shown in Fig. 5(a, b). Because of an alternate generation of vortex shedding, the drag and lift coefficients are showing periodic behavior. Energy spectrum of shear layer reattachment flow mode is displayed in Fig. 6(a). Strouhal number has widely spread single peak with very low frequency magnitude. It attained the value almost greater than 280. This represents that the weak vortices are formed at downstream position of channel.

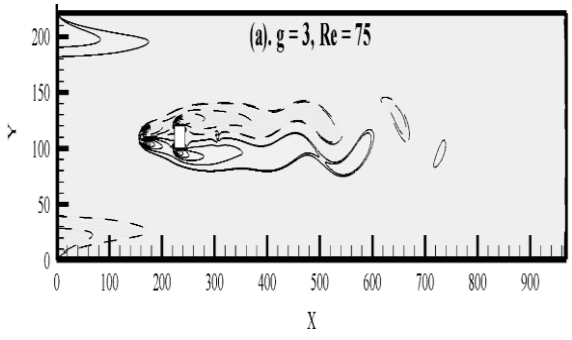

Fig4(a). *Vorticity contours visualization for shearlayer reattachment flow mode.*

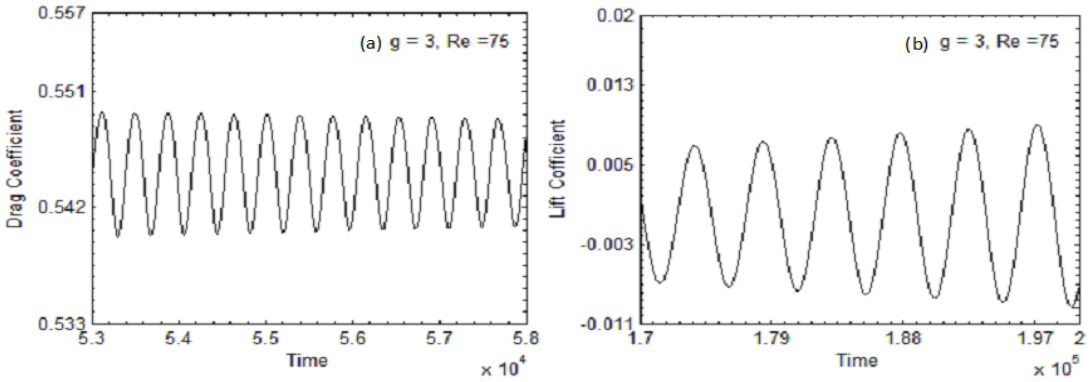

Fig5(a, b). *Time-Trace analysis of drag and lift coefficients for shearlayer reattachment flow mode*

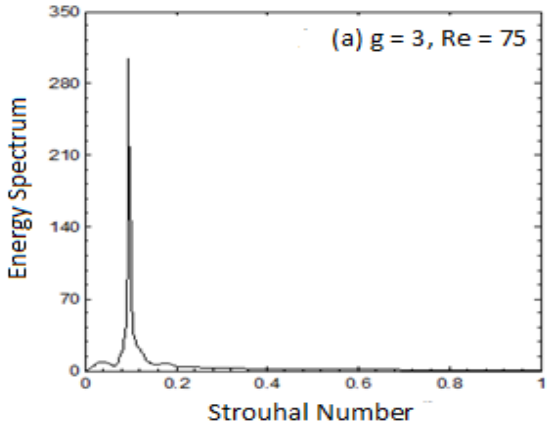

Fig6(a). *Energy spectrum analysis of lift coefficient for shearlayer reattachment flow mode*

Unsteady Flow Mode

Unsteady flow mode is observed at g = 1 for Re = 75 and at g = 4 for Re = 70 and 75, that is displayed in Fig. 7(a-c). At early stage of Re = 75 and g = 1, a visible change in fluid flow is observed at downstream location and vortices are formed in an alternate style by increasing the wake region. When gap is fixed at g = 4 and Re = 70, 75,but flow didn't pass within the gap between the main rod and both up and downstream control rods. After passing over downstream control rod, fluid flow made a small wake region and quickly produced the vortices towards the downstream side of the channel Fig. 7(b, c). Time-traces of drag and lift coefficients for g = 1 at Re = 75 and g = 4 at Re = 70 and 75 are shown in Fig. 8(a-f). Drag coefficient for g = 1and Re = 75 has periodic behavior because the vortices are generated in the alternate style, while lift coefficient has periodic as well as sinusoidal behavior Fig. 8(d, e). Drag and lift coefficient of g = 4 at Re = 70 has periodic behavior. Whereas, for g = 4 at Re = 75 drag coefficient has modulated behavior because the vortices are having high energy and greatest magnitude. Lift coefficient has periodic behavior (see Fig.8(e, f)).

Frequency magnitude of lift coefficient is studied by energy spectrum graph shown in Fig. 9(a-c). For g = 1 at Re = 75, energy spectrum has single peak and frequency magnitude is not very high due to weak vortex shedding shown in Fig. 9(a). When g = 4 at Re = 70, 75, the Strouhal number has single peak. It attained the high frequency magnitude as compared to g = 1 for Re = 75. This high magnitude shows that the vortices are propagated towards exit position with greatest energy level.

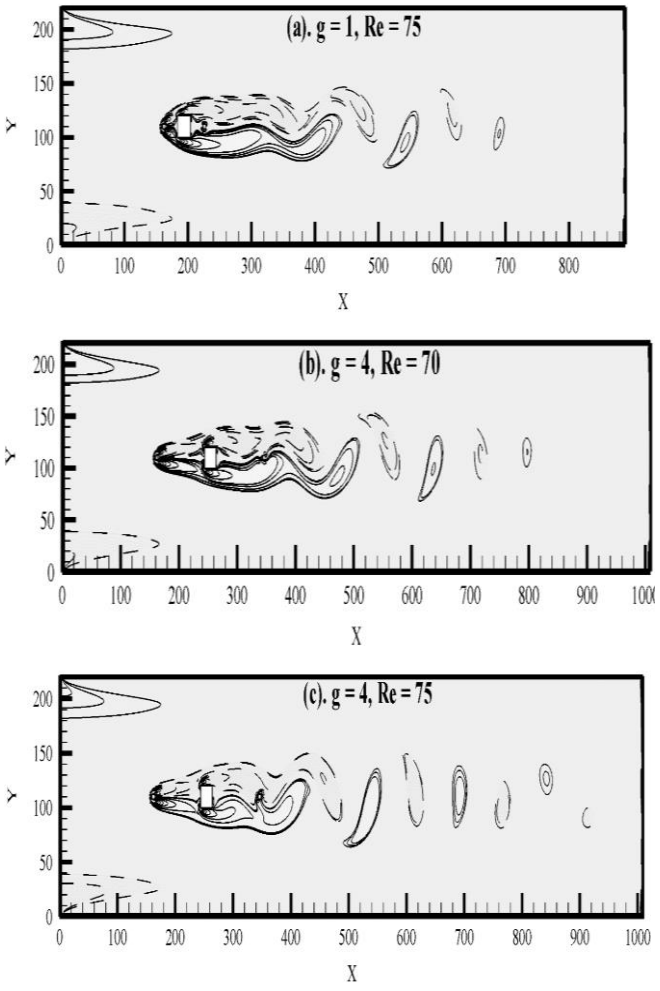

Fig5(a-c). *Vorticity contours visualization for unsteady flow mode.*

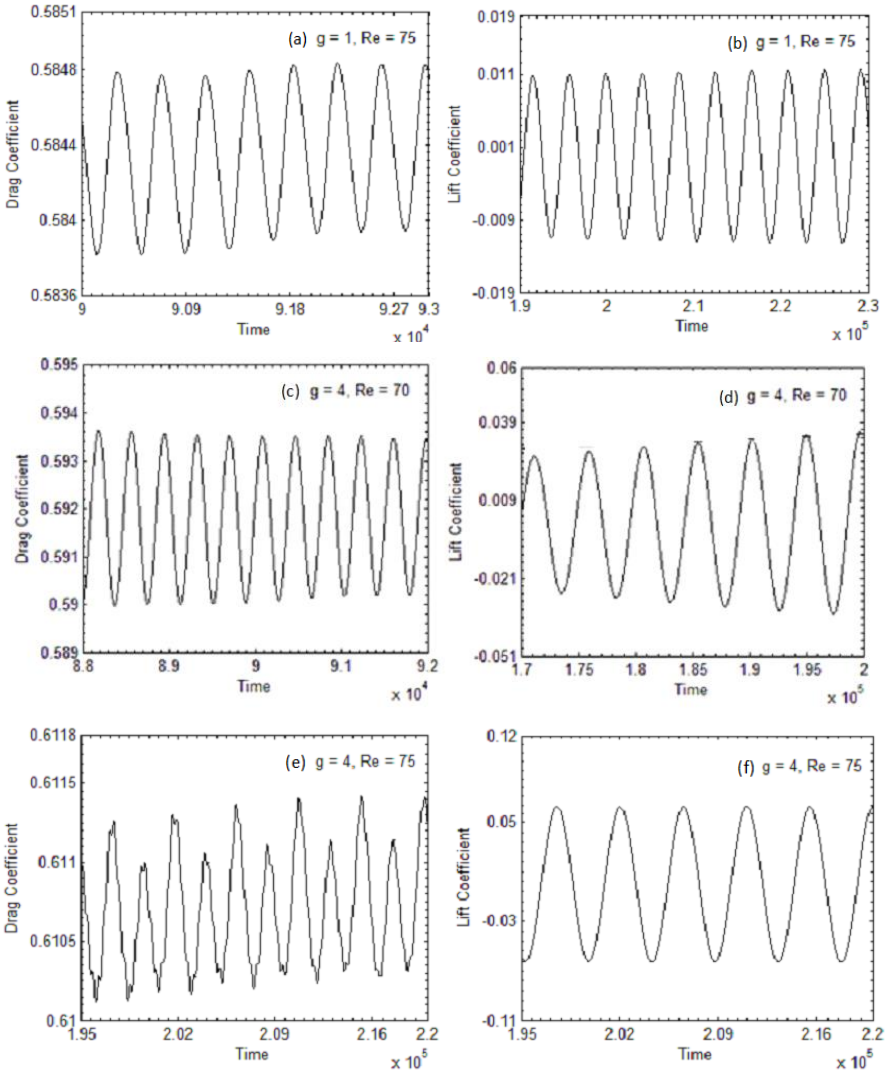

Fig8(a-f). *Time-Trace analysis of drag and lift coefficients for unsteady flow mode*

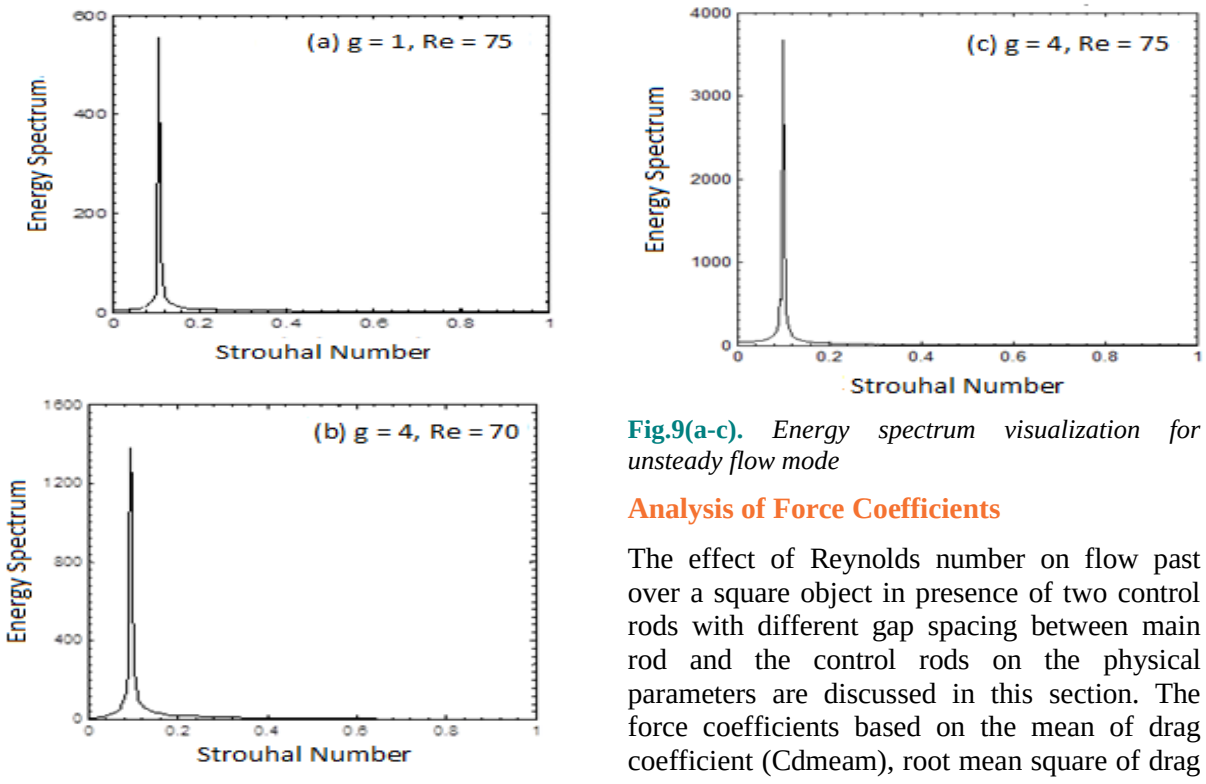

Fig.9(a-c). *Energy spectrum visualization for unsteady flow mode*

Analysis of Force Coefficients

The effect of Reynolds number on flow past over a square object in presence of two control rods with different gap spacing between main rod and the control rods on the physical parameters are discussed in this section. The force coefficients based on the mean of drag coefficient (Cdmeam), root mean square of drag

coefficient (Cdrms), root mean square of lift coefficient (Clrms) and Strouhal number (St) that are displayed in Fig. 10(a-d) and also mentioned in Table 4. The behaviors of these physical parameters are compared with single rod data. Straight black line is representing the numerical data for single rod and the lines with different symbols and colors are representing the present physical parameter's data with fixed gap at different Re = 1, 5, 10, 15, 20, 30, 40, 50, 55, 60, 70, 75. Fig. 10(a) representing the magnitude of Cdmean at different Reynolds numbers. For g = 1 at Re =1, Cdmean jumped at extreme point and attained its maximum value that is 5.5909, where steady flow mode is observed. This is greater than the value of single rod Cdmean. The point is to be noticed, that at small Reynolds number, Cdmean shoots up for all gap spacings but as Re is increased, Cdmean is seemed to be decreased and approached towards its minimum value at g = 2 for Re = 75. The minimum value of current Cdmean is 0.5293, where steady flow mode is occurred. In comparison with single rod Cdmean, the value of present Cdmean is greater than single rod Cdmean value when Re = 1 for all gaps. Later on, when Re is increased, the Cdmean of main rod become smaller and smaller (see Fig. 10(a)).Root mean square of drag coefficient (Cdrms) is displayed in Fig. 10(b). It is cleared that Cdrms value is smaller than single rod data for all gaps and Reynolds. Cdrms increased at g = 1 for Re = 5, but again it decreased at all selected gaps and Reynolds number. At (g, Re) = (3, 75) and (g, Re) = (4, 50), Cdrms is showing some increasing jumps and then finally Cdrms attained its maximum value at g = 3 for Re = 75, which is 0.383. Here Shearlayer reattachment flow mode is observed. The behavior of root mean square of lift coefficient (Clrms) is shown in Fig. 10(c). All values of Clrms in presence of control rods are smaller than single rod Clrms value. Clrms is representing the same behavior for g = 1-3 at Re = 1, 5, 10, 15, 20, 30, 40, 50, 55, 60 70 and 75. When Clrms is investigated for g = 4 and Re = 70, 75, it represents some fluctuations shown in Fig. 10(c). The maximum value of Clrms is 0.0375 obtained at g = 4 for Re = 75, where unsteady flow mode is occurred. Strouhal number is also important physical parameter that is graphically shown in Fig. 10(d). In comparison with single rod Stvalue, the St value in presence of control rods has smaller value than single rod St value. When Re is small and flow is steady, it has zero magnitude. As g is increased with increasing Reynolds number, the frequency of Strouhal number is changing. At g = 2, 3 and 4, Strouhal shoot upward in same style for Re = 40, 55 and 60. The maximum value of St is found at g = 1 for Re = 75 which is 0.1049, where unsteady flow mode is observed.

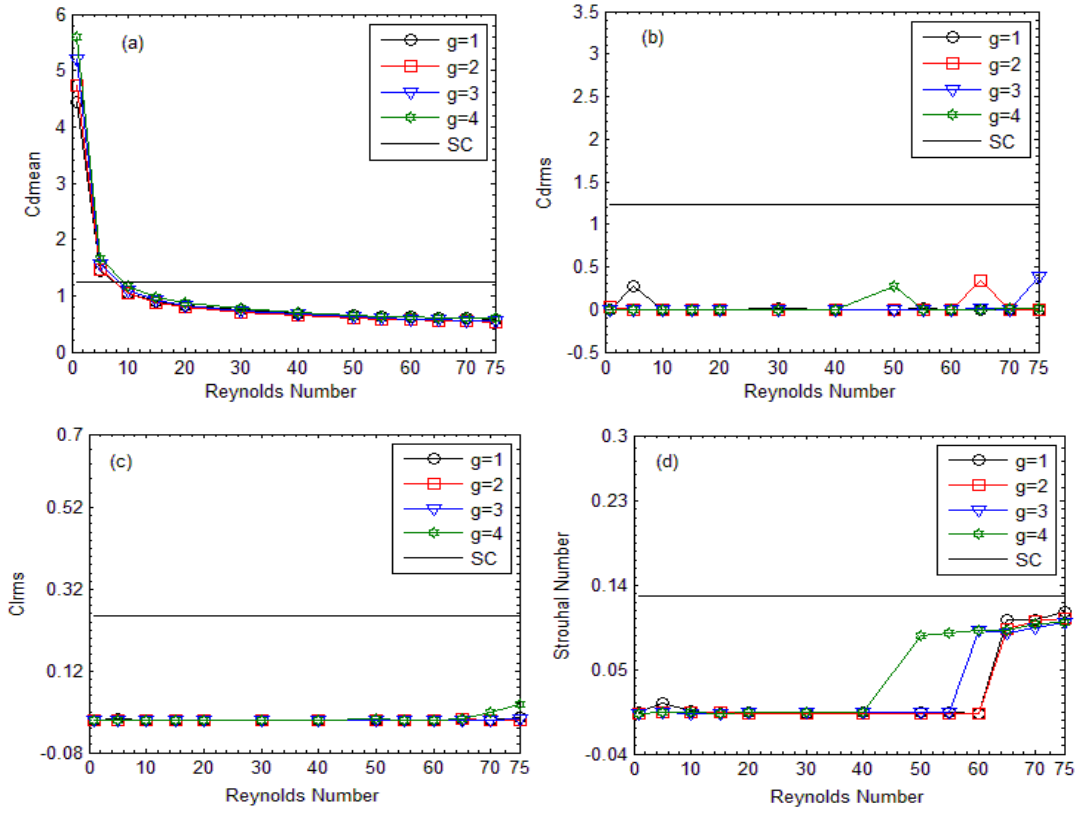

Fig10(a-d). *Analysis of force coefficients at fixed gap spacing by varying Reynolds number*

Table4. *Values of Physical parameters at g = 1- 4 at different Reynolds numbers*

g = 1												
Re	1	5	10	15	20	30	40	50	55	60	70	75
Cdmean	4.45	1.44	1.049	0.91	0.83	0.74	0.69	0.65	0.63	0.619	0.595	0.589
Cdrms	0	0	0	0	0	0.01	0	0.0001	0.0165	0.0001	0.0001	0.0030
Clrms	0	0	0	0	0	0	0	0	0.00001	0.000001	0.0003	0.006
St	0.004	0.014	0.006	0.003	0.004	0.003	0.004	0.0041	0.0041	0.0029	0.103	0.112
g = 2												
Re	1	5	10	15	20	30	40	50	55	60	70	75
Cdmean	4.731	1.467	1.043	0.884	0.798	0.699	0.64	0.600	0.583	0.568	0.541	0.529
Cdrms	0.033	0	0	0	0	0	0.0001	0.0002	0.0002	0.0002	0.0002	0.0002
Clrms	0	0	0	0	0	0	0	0.000002	0.0002	0.0000021	0.00014	0.0001
St	0.003	0.004	0.004	0.003	0.003	0.003	0.003	0.003	0.003	0.0029	0.102	0.105
g = 3												
Re	1	5	10	15	20	30	40	50	55	60	70	75
Cdmean	5.198	1.571	1.105	0.931	0.840	0.728	0.67	0.621	0.603	0.586	0.558	0.556
Cdrms	0	0	0	0	0.000031	0.0001	0.0002	0.0002	0.00024	0.00025	0.0003	0.383
Clrms	0	0	0	0	0	0	0	0.000002	0.000003	0.000008	0.00043	0.0038
St	0.003	0.0041	0.003	0.003	0.0041	0.0041	0.0041	0.0041	0.0041	0.0923	0.094	0.099
g = 4												
Re	**1**	**5**	**10**	**15**	**20**	**30**	**40**	**50**	**55**	**60**	**70**	**75**
Cdmean	5.60	1.66	1.167	0.982	0.882	0.768	0.702	0.658	0.637	0.620	0.599	0.603
Cdrms	0	0	0	0.00002	0.00003	0.00013	0.00023	0.2722	0.0003	0.00037	0.0091	0.0097
Clrms	0	0	0	0	0	0	0.000003	0.0015	0.000013	0.00011	0.019	0.0375
St	0	0	0	0	0	0	0	0.0863	0.0884	0.0920	0.0986	0.1004

CONCLUSIONS

Two dimensional numerical simulations have been performed by employing single-relaxation-time lattice Boltzmann method, to study the fluid flow behavior under the effect of different Reynolds numbers and gap spacing. The gap spacings between the main and dual control rods are taken as g = 1- 4 and Reynolds number is taken within the range Re = 1, 5, 10, 15, 20, 30, 40, 50, 55, 60, 70, 75. During this study, three type of flow modes are observed and named them as (i). Steady flow mode (ii). Shearlayer reattachment flow mode and (iii). Unsteady flow mode according to their behavior. The steady flow style is observed at g = 1, 3 for Re = 1-70, at g = 2 for Re = 1-75 and g = 4 for Re = 1-60. Shearlayer reattachment flow mode is occurred at g = 3 for Re = 75. While, unsteadiness in flow is observed only at g = 1 for Re = 75 and g = 4 for Re = 70 and 75. In physical parameters, Cdmean, Cdrms, Clrms and St values are calculated and compared with single rod data. At g = 1 and Re =1, Cdmean jumped at once and attained its maximum value that, is 5.5909 where existing flow mode is steady. The minimum value of Cdmean is 0.5293. Cdrms attained the maximum value at g = 3 for Re = 75, which is 0.3831, where Shearlayer reattachment flow mode is observed. Clrms values are approximately same at different Reynolds number, except at g = 4 and Re = 75, which increases regularly. The maximum value of Clrms is 0.0375occurred at g = 4 for Re = 75 with unsteady flow mode. The values of St are shown in Fig 9(4), which are having mixed behavior. That is increasing or decreasing with Re. It gained its maximum value at g = 1 for Re = 75 which is 0.1049, where unsteady flow mode is observed.

Nomenclature:

Cd drag coefficient

Cl lift coefficient

Cdmean mean drag coefficient

Cdrms root-mean-square value of drag coefficient

Clrms root-mean-square value of lift coefficient

FVM Finite volume method

d size of main cylinder

d1 size of control cylinders

F_d in-line force component

e_i velocity directions

f_i particle distribution function

$f_i^{(eq)}$ equilibrium distribution function

f_s vortex shedding frequency

g gap spacing

H height of the computational domain

L length of the computational domain

Ld downstream position

Lu upstream position

Q number of particles

Re Reynolds number

s surface-to-surface distance between cylinders

St Strouhal number

SSR Single square rod

U_∞ uniform inflow velocity

w_i weighting coefficients

Greek Symbols

τ relaxation-time

ν kinematic viscosity

ρ fluid density

REFERENCE

[1] V. Mansingh, P. H. Oosthuizen, "Effects of control plates on the wake flow behind a bluff body"*AIAA Journal*, 28, 778-783, (1990).

[2] H. Sakamoto, K. Tan, N. Takeuchi, H. Haniu, "Suppression of fluid forces acting on a square prism by passive control" *Journal of Fluids and Engineering*, 119, 506-511, (1997).

[3] S. Chen, G. Doolen, "Lattice Boltzmann method for fluid flows" *Annual Review of Fluid Mechanics*, 30, 329-364, (1998).

[4] C. Dalton, Y. Xu, J.C. Owen, "The suppression of lift on a Circular Rod Due to Vortex Sheddingat Moderate Reynolds Numbers" *Journal of Fluids Structure*, 15, 617-628, (2001).

[5] S. Mittal, "Effect of a "slip" control plate on vortex shedding from a rod" *Physics of Fluids*, *15*(3), 817-820, (2003).

[6] J.Y. Hwang, K.S. Yang, "Drag reduction on a circular rod using dual detached control plates" *Journal of Wind Engineering and Industrial Aerodynamics*, *95*(7), 551-564, (2007).

[7] C.P. Shao, Q.D. Wei, "Control of vortex shedding from a square rod," *AIAA Journal*, 46, 397-407, (2008).

[8] M.S.M. Ali, M.S.M., C.J. Doolan, V. Wheatley, "Aeolian tones generated by a square rod with a control plate" *Proceedings of 20th International Congress on Acoustics, ICA. Cidney Australia*, 1-8, (2010).

[9] M. S. M. Ali, C. J. Doolan, V. Wheatley, "Low Reynolds number flow over a square rod with a control plat" *Physics of Fluids*, *23*(3), 033602, (2011).

[10]H. Wu, D. P. Sun, L. Lu, B. Teng, G. Q. Tang, J. N. Song, "Experimental investigation on the suppression of vortex-induced vibration of long flexible riser by multiple control rods" *Journal of Fluids and Structures*, 30, 115-132, (2012).

[11]D. A. Perumal, V. S. Kumar, K. A. Dass, "Numerical simulation of viscous flow over a square cylinder using lattice Boltzmann method" *ISRN Mathematical Physics*, 1-16, (2012).

[12]S. Malekzadeh, A. Sohankar, "Reduction of fluid forces and heat transfer on a square rod in a laminar flow regime using a control plate" *International Journal of Heat and Fluid Flow*, 34, 15-27, (2012).

[13]R. Golani, A. K. Dhiman, "Fluid flow and heat transfer across a circular cylinder in the unsteady flow regime" *International Journal of Engineering Science*, 3(3), 8-19, (2014).

[14]L. Liu, M. Liu, B. Teng, Z. D. Cui, G. Q. Tan., M. Zhao, L. Cheng, " Numerical investigation of fluid flow past circular rod with multiple control rods at low Reynolds" *Journal of Fluids Structure*,48, 235-259, (2014).

[15]G.R. Vamsee, M.L. De Tena, S. Tiwari, "Effect of arrangement of inline control plate on flow past square rod" *Progress in Computational Fluid Dynamics*, 14, 277-293, (2014).

[16]B. Barman, S. Bhattacharyya, "Control of vortex shedding and drag reduction through dual control plates attached to a square rod" *Journal of Marine Sciences and their Applications*, 14,138-145, (2015).

[17]P. Dey, A. K. Das, "Numerical analysis of drag and lift reduction of square rod" *Engineering Science and Technology, An International Journal*, 18(4), 758-768, (2015).

[18]K. Nidhul, A. S. Sunil,V. Kishore, "Numerical investigation of flow characteristics over a square rod with detached flat plate of varying thickness at critical gap distance in the wake at low Reynoldsnumber" *International Journal of Research in Aeronautical and Mechanical Engineering*, 3(1), 104-118, (2015).

[19]S. U. Islam, R. Manzoor, Z. C. Ying, M. M. Rashdi, A. Khan,"Numerical investigation of fluid flow past a square rod using upstream, downstream and dual splitter plates" *Journal of Mechanical Science and Technology*, *31*(2), 669-687, (2017).

[20]S. U. Islam, R. Manzoor, U. Khan, G. Nazeer, S. Hassan, "Drag reduction on a square cylinder using multiple detached control cylinder" *KSCE Journal of Civil Engineering*, 22, 2023-2034, (2017).

[21]Z. Guo, H. Liu, L. S. Luo, K. Xu, "A comparative study of the LBE and GKS methods for 2-Dnear incompressible laminar flows" *Journal of Computational Physics*, 227(10), 4955-4976, (2008).

[22]M. Breuer, J. Bernsdorf, T. Zeiser, F. Durst, "Accurate computations of the laminar flow past a square rod based on two different methods: lattice-Boltzmann and finite-volume"

International Journal of Heat and Fluid Flow, 21, 186-196, (2000).

[23] D. Yu, R. Mei, L. S. Luo, W. Shyy, "Viscous flow computations with the method of lattice Boltzmann equation" *Progress in Aerospace Sciences*, 39, 329-367, (2003).

A. A. Mohammad, "Lattice Boltzmann Method: Fundamentals and Engineering Applications with Computer Codes" *Springer*, (2011).

[24] D. A. Wolf-Gladrow, "Lattice-Gas Cellular Automata and Lattice Boltzmann Models-An introduction" *Lecture Notes in Mathematics, 1725, Springer-Verlag, Berlin*, (2005).

[25] L. Zhou, M. Cheng, K.C. Hung, "Suppression of fluid force on a square rod by flow control" *Journal of Fluids Structure*, 21,151-167, (2005).

Citation: *Raheela Manzoor, Aneela Anwar, Shams-ul-Islam and Khurshid Jami, "Transition of Flow past a Square Rod through Passive Control Method at Low Reynolds Number", International Journal of Emerging Engineering Research and Technology, 8(6), 2020, pp. 32-43.*